

Novel *RP11L1* Variants and Genotype–Photoreceptor Microstructural Phenotype Associations in Cohort of Japanese Patients With Occult Macular Dystrophy

Kaoru Fujinami,^{1–3} Shuhei Kameya,⁴ Sachiko Kikuchi,⁴ Shinji Ueno,⁵ Mineo Kondo,⁶ Takaaki Hayashi,⁷ Kei Shinoda,⁸ Shigeki Machida,^{9,10} Kazuki Kuniyoshi,¹¹ Yuichi Kawamura,¹² Masakazu Akahori,¹² Kazutoshi Yoshitake,¹² Satoshi Katagiri,⁷ Ayami Nakanishi,⁵ Hiroyuki Sakuramoto,¹¹ Yoko Ozawa,² Kazuo Tsubota,² Kunihiko Yamaki,⁴ Atsushi Mizota,⁸ Hiroko Terasaki,⁵ Yozo Miyake,¹³ Takeshi Iwata,¹² and Kazushige Tsunoda¹

¹Laboratory of Visual Physiology, Division for Vision Research, National Institute of Sensory Organs, National Hospital Organization, Tokyo Medical Center, Meguro-ku, Tokyo, Japan

²Department of Ophthalmology, Keio University School of Medicine, Shinjyuku-ku, Tokyo, Japan

³UCL Institute of Ophthalmology, London, United Kingdom

⁴Department of Ophthalmology, Nippon Medical School Chiba Hokusoh Hospital, Inzai, Chiba, Japan

⁵Department of Ophthalmology, Nagoya University Graduate School of Medicine, Showa-ku, Nagoya, Aichi, Japan

⁶Department of Ophthalmology, Mie University Graduate School of Medicine, Tsu, Mie, Japan

⁷Department of Ophthalmology, The Jikei University School of Medicine, Nishi-Shimbashi, Minato-ku, Tokyo, Japan

⁸Department of Ophthalmology, Teikyo University School of Medicine, Itabashi-ku, Tokyo, Japan

⁹Department of Ophthalmology, Iwate Medical University School of Medicine, Morioka, Iwate, Japan

¹⁰Department of Ophthalmology, Dokkyo Medical University Koshigaya Hospital, Koshigaya, Saitama, Japan

¹¹Department of Ophthalmology, Kinki University Faculty of Medicine, Osaka-Sayama City, Osaka, Japan

¹²Division of Molecular and Cellular Biology, National Institute of Sensory Organs, National Hospital Organization, Tokyo Medical Center, Meguro-ku, Tokyo, Japan

¹³Aichi Medical University, Nagakute, Aichi, Japan

Correspondence: Kazushige Tsunoda, Division for Vision Research, National Institute of Sensory Organs, National Hospital Organization, Tokyo Medical Center, 2-5-1 Higashi-gaoka, Meguro-ku, Tokyo 152-8902, Japan; tsunodakazushige@kankakuki.go.jp.

KF and SKam contributed equally to the work presented here and should therefore be regarded as equivalent authors.

Submitted: March 31, 2016

Accepted: July 24, 2016

Citation: Fujinami K, Kameya S, Kikuchi S, et al. Novel *RP11L1* variants and genotype–photoreceptor microstructural phenotype associations in cohort of Japanese patients with occult macular dystrophy. *Invest Ophthalmol Vis Sci*. 2016;57:4837–4846. DOI:10.1167/iovs.16-19670

PURPOSE. To determine the clinical and genetic characteristics of Japanese patients with occult macular dystrophy (OMD) in a nationwide multicenter study.

METHODS. Twenty-three patients from 21 families with clinically diagnosed OMD were studied at 10 institutions throughout Japan. Ophthalmologic examinations including spectral-domain optic coherence tomography were performed. Patients were classified into two phenotype groups: a classical group having both blurred ellipsoid zone and absence of interdigitation zone of the photoreceptors, and a nonclassical group lacking at least one of these two features. Whole-exome sequencing, direct sequencing, and in silico molecular analysis were performed to detect the pathogenic *RP11L1* variants. Statistical associations between the phenotype and genotypes based on the presence of pathogenic *RP11L1* variants were investigated.

RESULTS. There were 12 families with the classical findings and 9 families with the nonclassical findings. Nine pathogenic *RP11L1* missense variants were identified in 12 families (57%) including three reported variants, namely, p.R45W, p.S1199C, and p.G1200A, and six novel variants, p.G221R, p.T1194M, p.T1196I, p.G1200D, p.G1200V, and p.V1201G. The pathogenic missense variants in seven families (33%) were located between amino acid numbers 1196 and 1201. A significant association was found between the photoreceptor microstructural phenotypes and molecular genotypes.

CONCLUSIONS. The spectrum of the morphologic phenotypes and pathogenic *RP11L1* variants was documented in a well-characterized Japanese cohort with OMD. A unique motif including six amino acids (1196–1201) downstream of the doublecortin domain could be a hot spot for *RP11L1* pathogenic variants. The significant association of the morphologic phenotypes and genotypes indicates that there are two types of pathophysiology underlying the occult macular dysfunction syndrome: a hereditary OMD with the classical phenotype (Miyake's disease), and a nonhereditary OMD-like syndrome with progressive occult maculopathy.

Keywords: ocular macular dystrophy, *RP11L1*, macular dystrophy, electroretinogram, Miyake's disease

Occult macular dystrophy (OMD; Online Mendelian Inheritance in Man [OMIM] 613587), first described by Miyake et al.¹⁻³ in 1989, is an inherited macular dystrophy characterized by a progressive decrease in the visual acuity in eyes with an essentially normal-appearing fundus and normal fluorescein angiograms. The full-field electroretinograms (ERGs) are usually normal; however, the focal macular ERGs, multifocal ERGs (mfERGs), and pattern ERGs are abnormal.⁴⁻⁷ These findings suggested that the retinal dysfunction is confined to the macula.⁴⁻⁷

Characteristic changes in the microstructure of the photoreceptors have been detected by spectral-domain optical coherence tomography (SD-OCT) in eyes with OMD, and these changes have been subsequently used in the diagnosis of OMD.^{3,8,9} The most prominent alterations in the SD-OCT images are the disruptions or absence of the two highly reflective lines in the macular area: the ellipsoid zone (EZ) and the interdigitation zone (IZ).^{3,8} The absence of the IZ at the fovea is the initial sign of this disorder.^{3,8,9} A thickened and blurred EZ in the early stage and disrupted or absent EZ in the late stage are common features of eyes with OMD.^{3,8} A thinning of the photoreceptor and outer nuclear layers becomes more apparent with increasing time, but the retinal pigment epithelium (RPE) remains unchanged.^{3,8}

In 2010, linkage analyses of two families with autosomal dominant inheritance OMD detected causative mutations in the retinitis pigmentosa 1-like 1 (*RP1L1*) gene (OMIM 608581).¹⁰ The *RP1L1* gene was originally identified by human and mouse genomes sequencing, and it contained four exons that span 50 kb on chromosome 8p.^{11,12} The *RP1L1* protein has a maximal length of 2,480 amino acids with a predicted molecular weight of 252 kDa. Immunohistochemistry showed that it is expressed in the rod and cone photoreceptors of cynomolgus monkeys.¹⁰ The *RP1L1* protein was suggested to be involved in the morphologic and functional maintenance of photoreceptors.^{3,11,13}

Since the discovery of the causative *RP1L1* mutations in patients with OMD, a number of OMD cases with *RP1L1* mutations have been reported.^{7,8,14-19} The most common mutation is c.133C>T, p.Arg45Trp in exon 2.^{7,8,10,15,17-19} In addition, extensive retinal dysfunction such as generalized cone dysfunction and generalized rod-cone dysfunction has been documented in patients with biallelic *RP1L1* gene aberrations.^{7,20,21} However, the spectrum of *RP1L1* variants and clinical characteristics of patients with OMD have not been completely determined because there have been no studies on a large cohort of patients with a definitive diagnosis of OMD in a specific population.

Thus, the purpose of this study was to determine the clinical and molecular genetic characteristics of a well-described cohort of patients with OMD in the Japanese population. This study also provided an opportunity to determine whether there was a significant association between the photoreceptor microstructures and the molecular genotypes in eyes with OMD.

METHODS

Patients

The protocol of this study adhered to the tenets of the Declaration of Helsinki and was approved by the Ethics Committee of the participating institutions: National Institute of Sensory Organs (NISO), National Hospital Organization, Tokyo Medical Center; Nippon Medical School Chiba Hokusoh Hospital; Nagoya University Graduate School of Medicine; Mie University Graduate School of Medicine; The

Jikei University School of Medicine; Teikyo University School of Medicine; Iwate Medical University School of Medicine; Kinki University Faculty of Medicine; and Aichi Medical University. A signed informed consent was obtained from all patients.

A cohort of 23 Japanese patients with clinically diagnosed OMD were studied between 2008 and 2012. All of the patients met the established criteria for the clinical diagnosis of OMD including a progressive decrease of the visual acuity in both eyes or a decrease of central vision, essentially normal fundus appearance, normal full-field ERGs, and localized macular dysfunction detected by focal macular or multifocal ERGs.¹⁻³ A full medical history with detailed family history was obtained from all.

Clinical Investigation, Data Uploading, and Morphologic Classification

Comprehensive ophthalmologic examinations were performed on all patients, and also on two unaffected family members who were used for cosegregation analyses (Fig. 1; subjects 2-II-2 and 7-II-1). The clinical evaluations included measurements of the best-corrected decimal visual acuity (BCVA), visual field testing, electrophysiological assessments, ophthalmoscopy, fundus autofluorescence (AF) imaging, and SD-OCT.^{1-3,5,8,9,22-24} All of the clinical data and images were uploaded into the NISO databank, and the diagnosis and data quality were confirmed by two of the authors (KF and KTsun).

The classical characteristic SD-OCT findings were defined as those in patients with the p.Arg45Trp mutation.^{3,8,10} All patients were classified into one of the two groups based on the microstructural changes of the photoreceptors: one group with the classical SD-OCT findings in which there was blurring of the EZ and absence of the IZ, and a second nonclassical group in which at least one of the two classical features was lacking.

Exome Sequencing, Targeted Analysis for Retinal Disease-Causing Genes on RetNET, and Variant Classification

After informed consents were obtained, blood samples were collected from the 23 patients and from two unaffected family members for cosegregation analyses.

Genomic DNA was extracted from the peripheral blood with the Genra Puregene Blood Kit (Qiagen, Tokyo, Japan) and sheared with the Covaris Ultrasonicator (Covaris, Woburn, MA, USA). Exome sequencing and targeted sequence analysis were done according to the published protocol of NISO, a customized analysis protocol for the Japanese population.^{25,26} Paired-end sequence library construction and exome capturing were performed by the Agilent Bravo automated liquid-handling platform with SureSelect XT Human All Exon kit V3-5 + UTRs kit (Agilent Technologies, Santa Clara, CA, USA). Enriched libraries were sequenced with the Illumina Hi-Seq2000 sequencer (San Diego, CA, USA; read length 2 × 101 bp).

Reads were aligned to the University of California, Santa Cruz, California, United States (USCS) human genome 19 reference sequence with Burrows-Wheeler Aligner software.²⁷ Duplicated reads were removed by Picard MarkDuplicates module, and mapped reads around insertion-deletion polymorphisms (INDELs) were realigned by the Genome Analysis Toolkit (GATK).²⁸ Base-quality scoring was recalibrated by GATK. Mutation calling was performed by the GATK Unified Genotyper module.

Called single-nucleotide variants (SNVs) and INDELs were annotated by the snpEff software (snpEff score; "high,"

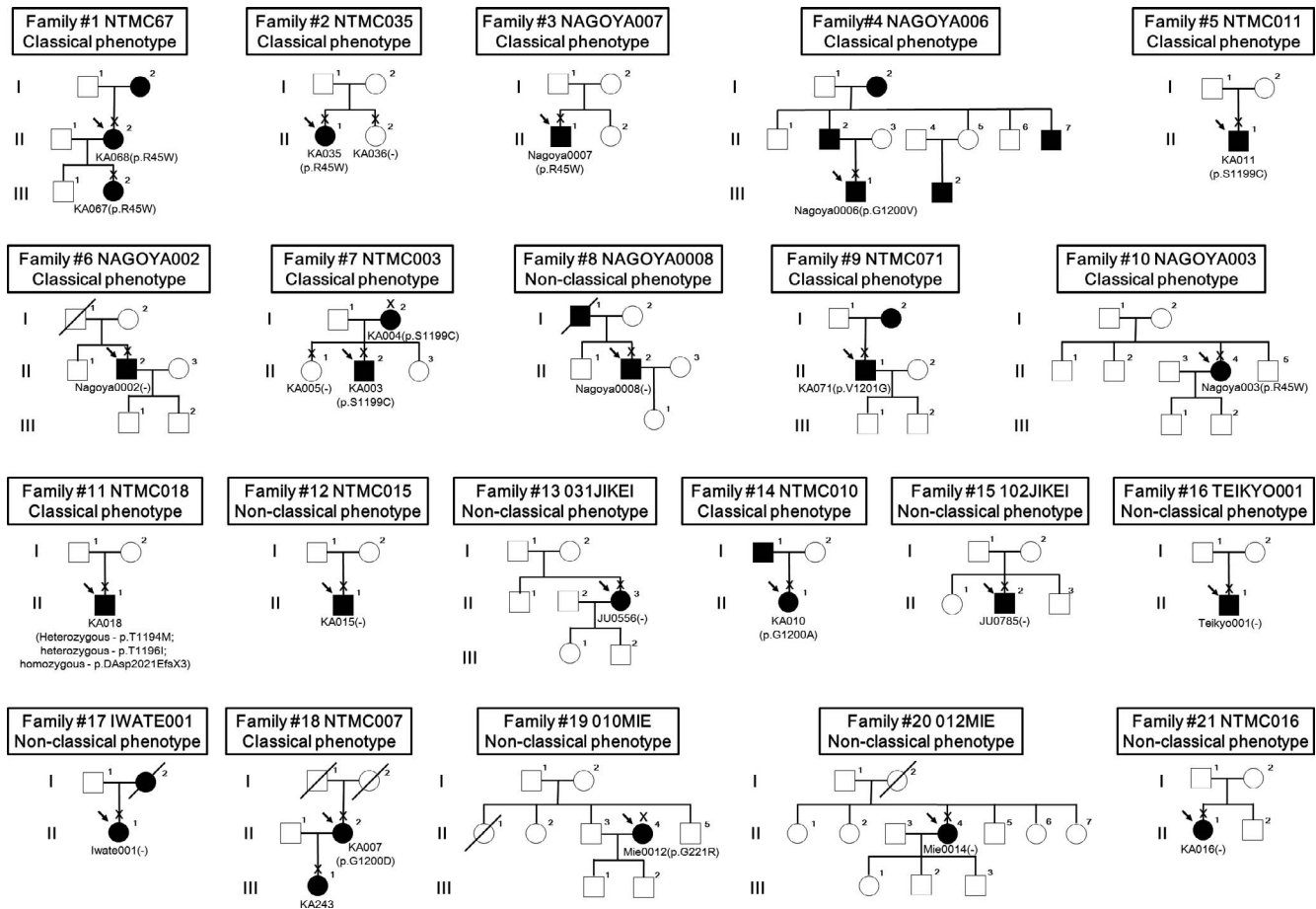


FIGURE 1. Pedigrees of 23 Japanese families with occult macular dystrophy (OMD). The *solid squares* (men) and *circles* (women) represent the affected patients. Unaffected family members are represented by *white icons*. The *slash symbol* indicates deceased individuals. The generation number is shown on the *left*. The proband of each pedigree is marked by an *arrow* and the clinically examined individuals are indicated by a *cross*.

“moderate,” or “low”).²⁹ All called SNVs and INDELS of the 238 genes registered as retinal disease-causing genes on the RetNet database were selected for further analysis (<https://sph.uth.edu/retnet/home.htm>; in the public domain). The identified variants were filtered with allele frequency (less than 1%) of the Human Genetic Variation Database (HGVD; <http://www.genome.med.kyoto-u.ac.jp/SnpDB/about.htm>; in the public domain), which is specific for the Japanese population. Depth and coverage for the targeted areas were interrogated using the integrative Genomics Viewer (<http://www.broadinstitute.org/igv/>; in the public domain).

Filtered variants were classified into two groups: variants with “high” damage predicted on SnpEff (major variants) and variants with “moderate” damage predicted on SnpEff (sub-major variants).

Direct Sequencing of *RP11* Gene

The *RP11* variants identified by exome sequencing and targeted analysis were further confirmed by direct sequencing in all patients and the two unaffected family members. The targeted exons, 2, 3, and 4, of the *RP11* gene were amplified by PCR using the established primer pairs (Transcript ID: NM_178857.5).^{14,20} Both DNA strands were sequenced by a sequencer, 3730xl DNA Analyzer using the BigDye Terminator kit V3.1 (Life Technologies Corporation, Carlsbad, CA, USA).^{14,20}

In Silico Molecular Genetic Analysis; Prediction, Frequency, and Conservation Scores

All identified variants were analyzed using three software prediction programs: SnpEff, Sorting Intolerant from Tolerant (SIFT; <http://sift.jcvi.org/>; in the public domain),³⁰ and PolyPhen2 (<http://genetics.bwh.harvard.edu/pph/index.html>; in the public domain).³¹

The allelic frequency of all of the variants was estimated with reference to two databases, the HGVD and the ExAC Browser (Beta; <http://exac.broadinstitute.org>; in the public domain).

Conservation in the positions of the identified variants was evaluated with primate PhyloP and phastCons scores provided by UCSC based on the human genome 19 coordinates.^{32,33} Higher PhyloP and phastCons scores were assigned to higher conservation.

Overall, the pathogenicity prediction of all variants, confirmed by direct sequencing, was classified into one of the two categories, pathogenic or less likely pathogenic, based on the results of software prediction, allelic frequency, and conservation score. Variants classified as pathogenic met three criteria: high pathogenicity on the prediction program (damaging on SIFT and probably damaging on Polyphen2 HDIV), low frequency (less than 1% on the ExAC Browser database for East Asian), and higher preservation score (more than 0.1 on PhyloP 46-way primate and 0.005 on Phast Cons 46-way primate).

TABLE 1. Key Phenotypic Features of 23 Affected Individuals With Occult Macular Dystrophy (OMD)

Fm ID	Pt ID	Inheritance	Sex	Age	Onset	BCVA		ERG			SD-OCT	
						RE	LE	Full Field	Central Dysfunction	Funduscopy	Blurring of EZ	Absence of IZ
1	1-III-2	AD	Female	14	7	0.8	0.7	Normal	(+)	Normal	(+)	(+)
1	1-II-2	AD	Female	45	40	0.15	0.3	Normal	(+)	Normal	(+)	(+)
2	2-II-1	Isolated	Female	31	25	0.2	0.2	Normal	(+)	Normal	(+)	(+)
3	3-II-1	Isolated	Male	36	20	0.3	0.6	Normal	(+)	Normal	(+)	(+)
4	4-III-1	AD	Male	46	33	0.15	0.2	Normal	(+)	Pale disc	(+)	(+)
5	5-II-1	Isolated	Male	42	34	0.2	0.2	Normal	(+)	Normal	(+)	(+)
6	6-II-2	Isolated	Male	42	38	0.2	0.1	Normal	(+)	Normal	(+)	(+)
7	7-II-2	AD	Male	49	48	0.3	0.2	Normal	(+)	Pale disc	(+)	(+)
7	7-I-2	AD	Female	79	79	0.3	0.2	Normal	(+)	Pale disc	(+)	(+)
8	8-II-2	AD	Male	48	30	0.3	0.2	Normal	(+)	Normal	(-)	(+)
9	9-II-1	AD	Male	51	25	0.1	0.2	Normal	(+)	Normal	(+)	(+)
10	10-II-4	Isolated	Female	52	48	0.2	0.2	Normal	(+)	Normal	(+)	(+)
11	11-II-1	Isolated	Male	52	45	0.7	0.1	Normal	(+)	Normal	(+)	(+)
12	12-II-1	Isolated	Male	52	44	0.5	0.4	Normal	(+)	Normal	(-)	(-)
13	13-II-3	Isolated	Female	58	53	1.2	1.2	Normal	(+)	Normal	(-)	(-)
14	14-II-1	AD	Female	54	40	0.08	0.1	Normal	(+)	Normal	(+)	(+)
15	15-II-2	Isolated	Male	64	62	0.1	0.2	Normal	(+)	Normal	(-)	(+)
16	16-II-1	Isolated	Male	57	47	0.2	0.2	Normal	(+)	Normal	(-)	(-)
17	17-II-1	AD	Female	58	48	0.4	0.3	Normal	(+)	Normal	(-)	(-)
18	18-II-2	AD	Female	65	61	0.5	0.5	Normal	(+)	Normal	(+)	(+)
19	19-II-4	Isolated	Male	69	64	0.6	0.6	Normal	(+)	Hard drusen	(-)	(-)
20	20-II-4	Isolated	Male	72	40	0.1	0.1	Normal	(+)	Normal	(-)	(+)
21	21-II-1	Isolated	Female	66	60	1	1	Normal	(+)	Normal	(-)	(+)

Autosomal dominant inheritance was confirmed by full clinical examinations in three families (families 1, 7, and 18). An autosomal dominant family history was found reported in five families (families 4, 8, 9, 14, and 17, by direct questioning). AD, autosomal dominant; Fm, family; LE, left eye; Pt, patient; RE, right eye.

Association Between Microstructural Phenotype Classification and Genotype Classification

All families were classified into one of two genotype groups based on the presence of pathogenic *RP11* variants: the *RP11*-positive group and the *RP11*-negative group.

Fisher's exact test was used to determine the significance of the association between the microstructural phenotype classification and genotype classification with commercially available software, Excel Tokei 2012 (Social Survey Research Information Co., Ltd., Tokyo, Japan). *P* values < 0.05 were considered statistically significant.

RESULTS

Demographics, Clinical Findings, and Photoreceptor Microstructural Classification

Twenty-three patients from 21 Japanese families with a clinical diagnosis of OMD were studied. The key phenotypic findings are shown in Table 1, and detailed clinical data are presented in Supplementary Table S1. The pedigree charts of the 21 families are shown in Figure 1. Autosomal dominant inheritance was confirmed by full clinical examinations in three families (families 1, 7, and 18), and an autosomal dominant family history was found in five families (families 4, 8, 9, 14, and 17) by direct questioning.

There were 10 women (43%) and 13 men (57%). The median age at the initial examination was 52.0 years with a range of 14 to 79 years, and the median age at the onset was 44.0 years with a range of 7 to 79 years. The decimal BCVA ranged from 0.08 to 1.2, and two patients had a BCVA of ≥ 1.0 in both eyes. All of the patients complained of decreased

central vision, and 15 had photophobia (15/23, 65%). The visual fields were determined in 17 patients; a central scotoma was detected in 16 patients (16/17, 94%), and no visual field defect was detected in 1 patient (1/17, 6%). There were two patients with normal-tension glaucoma and glaucoma-associated visual field defects (2/17, 12%).

Electrophysiological recordings showed localized macular dysfunction in all patients. A pale optic disc was detected in three patients (3/23, 13%), and hard drusen was found in one patient (1/23, 4%). One patient had an epiretinal membrane in the left eye, and the affected eye was excluded from all the imaging analyses. The AF images were normal in 14 patients (14/23, 61%); there were hyperautofluorescent changes in the parafoveal area in 5 patients (5/23, 22%), and a ring AF enhancement at the foveola in 4 patients (4/23, 17%).

Spectral-domain OCT showed that the IZ was not present in 18 patients (18/23, 78%) and blurred EZ was detected in 14 patients (14/23, 61%). There were five patients (5/23, 22%) who had neither absence of IZ nor blurred EZ. None of the patients had RPE atrophy. Representative SD-OCT images from 10 subjects are shown in Figure 2.

Exome Sequencing Analysis and Candidate Variant Detection

Exome sequencing and targeted analysis were performed on all 23 affected individuals and two unaffected family members. Adequate data quality was verified and proper analysis was performed on all of the subjects (Supplementary Table S2). After filtration, 13 variants were identified in the *RP11* gene by targeted exome analysis in the 23 patients (Table 2). *RP11* variants were detected in 16 patients from 14 families. No variant was found in seven patients from seven families.

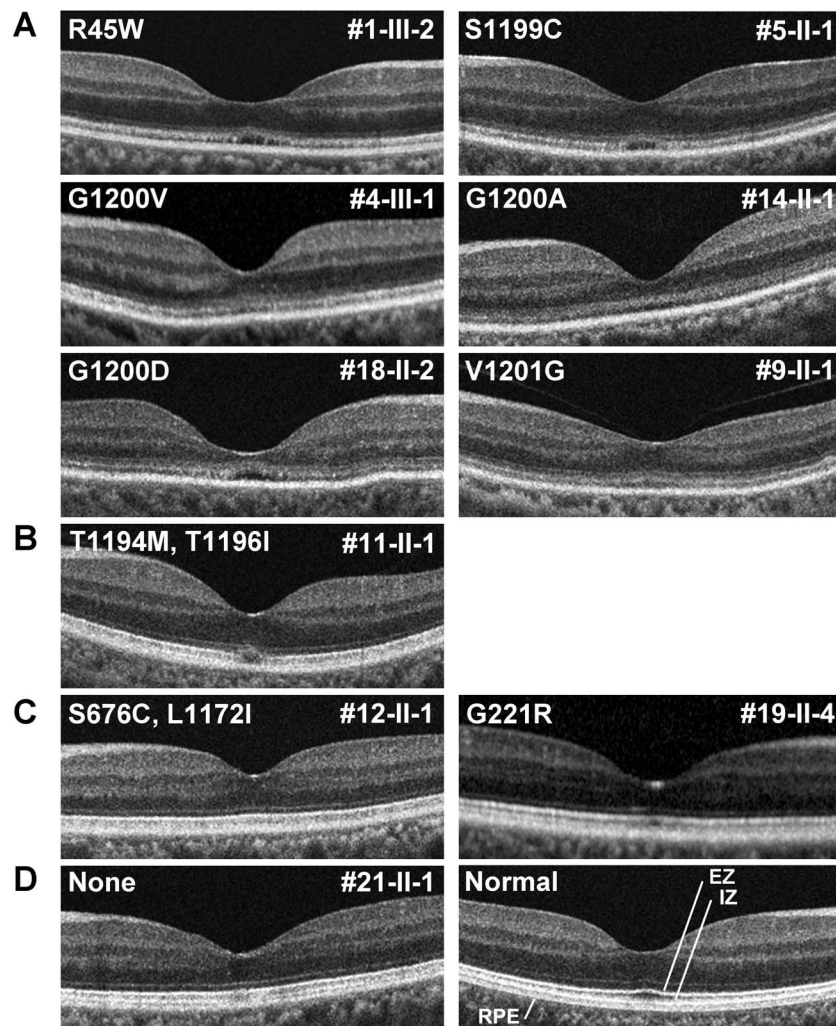


FIGURE 2. Spectral-domain optical coherence tomographic (SD-OCT) images of representative cases of OMD. Mutant amino acid changes and patient's ID are shown in the *upper left* and *upper right*, respectively. **(A)** Spectral-domain OCT images of six patients showing the classical photoreceptor microstructural findings with blurred ellipsoid zone (EZ) and absence of the interdigitation zone (IZ) with pathogenic missense *RP11* mutations. **(B)** Spectral-domain OCT image from a patient with classical photoreceptor microstructural findings and two missense mutations in cis. **(C)** Spectral-domain OCT images of two patients having the nonclassical microstructural findings: one patient with a less likely pathogenic *RP11* variant (12-II-1) and the other with a pathogenic missense mutation (19-II-4). **(D)** Spectral-domain OCT image of a *RP11*-negative patient showing the nonclassical microstructural findings and normal control. Definition of the highly reflective lines in the SD-OCT images shown in a normal control eye. EZ, ellipsoid zone; IZ, interdigitation zone; RPE, retinal pigment epithelium.

Direct Sequencing of 13 Candidate *RP11* Variants Identified by Exome Analysis

Direct sequencing of the other 13 variants detected by targeted exome analysis was performed, and all of these variants were verified (Table 2). Cosegregation analysis with unaffected family members in terms of the candidate variants was performed in two families (family 2, c.133C>T, p.Arg45Trp; family 7, c.3596C>G, p.Ser1199Cys). These variants were not detected in the unaffected family members.

Detection of Disease-Causing Variants With In Silico Molecular Genetic Analysis

A summary of the results of the in silico molecular genetic evaluations of the variants identified by exome analysis is presented in Table 3. Nine missense variants met the criteria and were classified as pathogenic. The pathogenic missense variants included three already reported variants, namely, c.133C>T, p.Arg45Trp; c.3596C>G, p.Ser1199Cys; and c.3599G>C,

p.Gly1200Ala. There were also six pathogenic variants that have not been reported, namely, c.661G>A, p.Gly221Arg; c.3581C>T, p.Thr1194Met; c.3581C>T, p.Thr1196Ile; c.3599G>T, p.Gly1200Val; c.3599G>A, p.Gly1200Asp; and c.3602T>G, p.Val1201Gly. Four variants were determined to less likely be pathogenic, namely, c.2026A>T, p.Ser676Cys; c.3514C>A, p.Leu1172Ile; c.4650T>G, p.Asn1550Lys; and c.6063delC, p.Asp2021Glu>Ter3.

Two missense variants, c.3581C>T, p.Thr1194Met and c.3587C>T, p.Thr1196Ile, were identified in a patient (11-II-1), and analysis of each exome sequence read with the integrative Genomics Viewer revealed that these two variants are located on the same chromosome (in cis). It is not possible to determine which of the variants are pathogenic or indeed if it is a combination of the two variants that leads to disease. However, there are 14 alleles comprising four different amino acid changes at the former position (p.Thr1194) present in the ExAC dataset. Furthermore, this residue exhibits incomplete conservation throughout mammalian *RP11* orthologues. Therefore the latter residue (c.3587C>T, p.Thr1196Ile), which is completely con-

TABLE 2. Summary of Detected Variants in *RP11* Gene of 23 Affected Individuals

Pt ID	Ex	Nucleotide and Amino Acid Changes Detected by Exome Analysis	Pos	State	Confirmation by Direct Sequencing
1-III-2	2	c.133C>T, p.Arg45Trp	10480579	Het	Confirmed
1-II-2	2	c.133C>T, p.Arg45Trp	10480579	Het	Confirmed
2-II-1	2	c.133C>T, p.Arg45Trp	10480579	Het	Confirmed
3-II-1	2	c.133C>T, p.Arg45Trp	10480579	Het	Confirmed
4-III-1	2	c.3599G>T, p.Gly1200Val	10468009	Het	Confirmed
5-II-1	4	c.3596C>G, p.Ser1199Cys	10468012	Het	Confirmed
6-II-2		Not detected			
7-II-2	4	c.3596C>G, p.Ser1199Cys	10468012	Het	Confirmed
7-I-2	4	c.3596C>G, p.Ser1199Cys	10468012	Het	Confirmed
8-II-2		Not detected			
9-II-1	4	c.3602T>G, p.Val1201Gly	10468006	Het	Confirmed
10-II-4	2	c.133C>T, p.Arg45Trp	10480579	Het	Confirmed
11-II-1	4	c.3581C>T, p.Thr1194Met	10468027	Het	Confirmed
	4	c.3587C>T, p.Thr1196Ile	10468021	Het	Confirmed
	4	c.6063delC, p.Asp2021GlufsTer3	10465544	Homo	Confirmed
12-II-1	4	c.2026A>T, p.Ser676Cys	10469582	Het	Confirmed
	4	c.3514C>A, p.Leu1172Ile	10468094	Het	Confirmed
13-II-3		Not detected			
14-II-1	4	c.3599G>C, p.Gly1200Ala	10468009	Het	Confirmed
	4	c.4650T>G, p.Asn1550Lys	10465544	Het	Confirmed
15-II-2		Not detected			
16-II-1		Not detected			
17-II-1		Not detected			
18-II-2	4	c.3599G>A, p.Gly1200Asp	10468009	Het	Confirmed
19-II-4	3	c.661G>A, p.Gly221Arg	10474046	Het	Confirmed
20-II-4		Not detected			
21-II-1		Not detected			

RP11 transcript ID, NM_178857.5. All the detected variants were in heterozygous status except for one variant in homozygous status (p.Asp2021GlufsTer3). Pt, patient; Ex, exon; Het, heterozygous; Homo, homozygous; Pos, position.

served throughout mammalian orthologues and unaltered in the ExAC dataset, may be more likely to be pathogenic if altered. This patient also had a homozygous frameshift variant with premature termination (c.6063delC, p.Asp2021GlufsTer3), which had relatively higher allele frequency and significantly lower conservation scores and was classified as less likely pathogenic: 0.5% in the normal Japanese population on HGVD and 0.174% of the East Asian population on ExAC; PhyloP and Phastcons scores of -1.11 and 0.02. It was uncertain whether this homozygous frameshift variant has a considerable clinical impact, since the missense variant, c.3587C>T, p.Thr1196Ile, is most likely disease causing in this patient.

Overall, 9 disease-causing variants were identified in 14 patients (14/23, 61%) from the 12 families (12/21, 57%). One common variant, c.133C>T, p.Arg45Trp, was detected in five patients from four families, and another common variant, c.3596C>G, p.Ser1199Cys, was found in three patients from two families. Six novel pathogenic variants were identified in five patients from five families (5/21, 26%). Of the nine pathogenic variants, six were located between amino acid numbers 1196 and 1201, which is downstream of the doublecortin domain.⁷

Major Variants of Other Retinal Disease-Causing Genes on RetNet

Among the nine patients without pathogenic *RP11* variants, two major variants of other retinal disease-causing genes were detected in the RetNet in three patients; c.5797C>T, p.Arg1933Ter of the *RPI* gene in two subjects and c.1023C>A, p.Tyr341Ter of the *RP2* gene in one subject (Table 4).

Association Between Photoreceptor Microstructural Phenotype Classification and Genotype Classification

All 23 patients were classified into one of the two groups based on the changes in the microstructures of the photoreceptors detected in the SD-OCT images. There were 14 patients in the classical group with both EZ blurring and IZ absence, and 9 patients in the nonclassical group with only one of the two microstructure abnormalities (Table 1). The classical SD-OCT findings were identified in 12 families and nonclassical findings in 9 (Tables 1, 5; Fig. 1). No discordance of the microstructural classification was found in the pedigrees of three families including multiple affected members (families 1, 7, and 18). Pathogenic *RP11* variants were detected in 12 families, and no pathogenic *RP11* variants were detected in 9 families. There was a significant association between the microstructural classification and genotype classification ($P = 0.000371$, Table 5).

Six of the eight families with autosomal dominant OMD inheritance or history were identified as having pathogenic *RP11* variants (6/8, 75%). All of these *RP11*-positive families had the classical SD-OCT findings, while two autosomal dominant families with nonclassical SD-OCT findings did not have *RP11* pathogenic variants (families 8 and 17, Fig. 1).

DISCUSSION

Our results indicated that there was a significant association between the genotype and the photoreceptor microstructural phenotype; that is, the presence of pathogenic *RP11* variants

TABLE 3. Results of In Silico Molecular Genetic Analysis of the Detected *RPL11* Variants

Fm ID	Ex	Nucleotide Change, Amino Acid Change	Allele Frequency, %						HGVD	Prediction		Conservation Score		Report	Pathogenicity
			EA	SA	EU	LA	AF	Total		SIFT/Polyphen2 HDIV	PhyloP	Phast Cons	dbSNP ID		
1, 2, 3, 10	2	c.133C>T, p.Arg45Trp	0.000	0.012	0.000	0.003	0.000	0.000	0.003	D/PROD	0.46	0.09	rs267607017	Akahori et al. ¹⁰	P
19	3	c.661G>A, p.Gly221Arg	0.000	0.000	0.000	0.009	0.000	0.001	0.001	D/PROD	0.46	0.16	rs767095509	This study	P
12	4	c.2026A>T, p.Ser676Cys	0.100	0.012	0.000	0.000	0.000	0.001	0.001	T/B	-1.60	0.02	rs752248086	Ahn et al. ¹⁸	LLP
12	4	c.3514C>A, p.Leu1172Ile	0.300	0.081	1.757	0.202	0.069	0.000	0.371	D/PROD	-0.30	0.01	rs143870426	This study	LLP
11	4	c.3581C>T, p.Thr1194Met	0.000	0.000	0.055	0.000	0.000	0.000	0.007	D/PROD	0.56	0.04	rs552391475	This study	P
11	4	c.3587C>T, p.Thr1196Ile	0.000	0.000	0.000	0.000	0.000	0.000	0.000	D/PROD	0.56	0.04	ND	This study	P
5, 7	4	c.3596C>G, p.Ser1199Cys	0.000	0.000	0.000	0.000	0.000	0.021	0.002	D/PROD	0.56	0.03	ND	Kabuto et al. ¹⁴	P
4	4	c.3599G>T, p.Gly1200Val	0.000	0.000	0.000	0.000	0.000	0.000	0.000	D/PROD	0.56	0.01	ND	This study	P
14	4	c.3599G>C, p.Gly1200Ala	0.000	0.000	0.000	0.000	0.000	0.000	0.000	D/PROD	0.56	0.01	ND	Davidson et al. ⁷	P
18	4	c.3599G>A, p.Gly1200Asp	0.000	0.000	0.000	0.000	0.000	0.000	0.000	D/PROD	0.56	0.01	ND	This study	P
9	4	c.3602T>G, p.Val1201Gly	0.000	0.000	0.000	0.000	0.000	0.000	0.000	D/PROD	0.46	0.01	ND	This study	P
14	4	c.4650T>G, p.Asn1550Lys	0.100	0.012	0.000	0.000	0.000	0.000	0.001	D/PROD	-1.73	0.00	rs760013790	This study	LLP
11	4	c.6063delC, p.Asp2021GlufsTer3	0.500	0.174	0.000	0.000	0.000	0.012	0.012	ND/ND	-1.11	0.02	rs572305644	This study	LLP

All identified variants were analyzed using three software prediction programs, SnpEff, Sorting Intolerant from Tolerant (SIFT; <http://sift.jcvi.org/>; in the public domain), and PolyPhen2 (<http://genetics.bwh.harvard.edu/pph/index.html>; accessed on September 1, 2015). The allelic frequency of all of the variants was estimated in reference to two databases, the HGVD (<http://www.genome.med.kyoto-u.ac.jp/SnpDB/about.htm>, in the public domain) and the ExAC Browser (Beta; <http://exac.broadinstitute.org>; in the public domain). Conservation in the positions of the identified variants was evaluated with primate PhyloP 46-way primate and phastCons 46-way primate scores provided by UCSC based on the human genome 19 coordinates (<http://genome.ucsc.edu/cgi-bin/hgTrackUi?db=hg19&g=cons46way>; in the public domain). Variants classified as pathogenic met three criteria: high pathogenicity on the prediction program (damage on SIFT and probably damaging on Polyphen2 HDIV), low frequency (less than 1% on the ExAC Browser database for East Asian), and higher preservation score (more than 0.1 on PhyloP 46way primate and 0.005 on Phast Cons 46way primate). Af, African; B, benign; D, damaging; EA, East Asian; Eu, European (non-Finish); Ex, exon; Hetero, heterozygous; Homo, homozygous; HGVD, human genetic variation database; La, Latino; LLP, less likely pathogenic; ND, not detected; P, pathogenic; PROD, probably damaging; SA, South Asian; T, tolerated.

TABLE 4. Two Major Variants of Retinal Disease-Causing Genes on RetNet Identified in *RP1L*-Negative OMD

Fm ID	Gene	Chr	Ex	Nucleotide Change, Amino Acid Change	Pos	State	HGVD	Allele Frequency, %					Phast Cons	dbsNP ID			
								ExAC							PhyloP	Conservation Score	
								EA	SA	EU	LA	AF					
6, 15	<i>RP1</i>	8	4	c.5797C>T, p.Arg1933Ter	55542239	Het	0.500	0.162	0.000	0.003	0.000	0.000	0.000	0.013	0.66	0.79	rs118031911
21	<i>RP2</i>	X	5	c.1023C>A, p.Tyr341Ter	46739174	Het	0.000	0.000	0.000	0.000	0.000	0.000	0.000	0.000	0.50	0.97	ND

RP1 transcript ID, NM_006269.1. RP2 transcript ID, NM_006915.2. Functional class of both variants was nonsense and classified as major. Af, African; B, benign; Chr, chromosome; D, damaging; EA, East Asian; EU, European (Non Finnish); Ex, exon; Fm ID, family ID; Hetero, heterozygous; HGVD, Human genetic variation database; La, Latino; P, Pathogenic; Pos, position; SA, South Asian.

TABLE 5. Association Between Photoreceptor Microstructural Phenotype Classification and Genotype Classification

Microstructural Classification	Pathogenic <i>RP1L1</i> Mutation, +	Pathogenic <i>RP1L1</i> Mutation, -
Classical, <i>N</i> = 12 families	11	1
Nonclassical, <i>N</i> = 9 families	1	8
Total, <i>N</i> = 21 families	12	9

All patients were classified into one of the two groups based on the microstructural changes of the photoreceptors: a group with the classical SD-OCT findings in which there was blurring of the EZ and absence of the IZ. The second group was the nonclassical group with at least one of the two classical features lacking. All families were classified into one of two genotype groups based on the presence of pathogenic *RP1L1* variants: the *RP1L1*-positive group and the *RP1L1*-negative group.

was significantly associated with an abnormality of both EZ blurring and IZ absence of the photoreceptor microstructures. Thus, patients presenting clinically with occult macular dysfunction syndrome can be separated into those with hereditary OMD caused by genetic mutations (including Miyake's disease; *RP1L1*-associated retinal disorder) and those with nonhereditary OMD-like syndrome with progressive occult maculopathy showing clinical signs resembling OMD.

Consistent changes of the photoreceptor microstructures were detected in the SD-OCT images in 11 of the 12 families in the pathogenic *RP1L1*-positive group (Fig. 1; Table 5). A concordance of the microstructural phenotype and the presence of pathogenic *RP1L1* variants was found in two families with pathogenic *RP1L1* mutations (families 1, 7). These findings are keeping with the fact that the mutations of the *RP1L1* gene result in specific damage in the photoreceptor microstructures in a unique manner.^{3,11,13,18} Our results therefore support the assumption that the *RP1L1* protein is involved in the morphologic and functional maintenance of photoreceptors.

The most common pathogenic variant, c.133C>T, p.R45W, was detected in five patients from four families in our study, which is a hot spot as previously reported.³ The missense pathogenic variants in seven patients were located between amino acid numbers 1196 and 1201, which is downstream of the doublecortin domain.⁷ In earlier reports, three pathogenic variants, p.S1199C, p.S1199P, and p.G1200A, were also located in this region.^{7,16} This six amino acid residue sequence (TSSSGV), which is highly conserved throughout mammalian orthologues²⁰ (NCBI HomoloGene; <http://www.ncbi.nlm.nih.gov/homologene>; in the public domain; accessed on June 1, 2016) and is absent from any other protein (UniProt; <http://www.uniprot.org/>; in the public domain; accessed on June 1, 2016), may therefore be considered a second mutation hot spot for OMD. Furthermore, these results indicate that this significantly unique motif could have an important function in the *RP1L1* protein.

There was still another pathogenic missense mutation, p.G221R, not found around the aforementioned hot spot regions. A patient (19-II-4) with this mutation had neither the EZ blurring nor IZ absence in the SD-OCT images. Two possibilities explain this atypical photoreceptor microstructural phenotype. One is that the patient is currently at a very early stage of OMD although he is 69 years old with an onset at 64 years of age. Another possibility is a limitation in the in silico prediction, which did not exclude this variant because the analysis was technically imperfect in evaluating the actual pathogenesis.

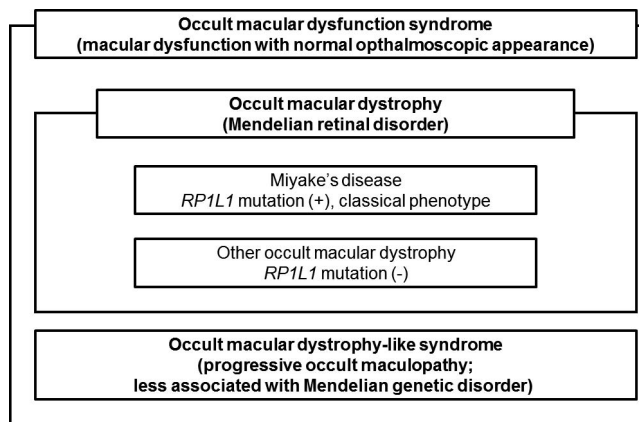


FIGURE 3. Classification of occult macular dysfunction syndrome. Occult macular dysfunction syndrome includes three subcategories: *RP1L1*-associated occult macular dystrophy (Miyake's disease), other hereditary occult macular dystrophy caused by other gene abnormalities, and nonhereditary occult macular dystrophy-like syndrome (progressive occult maculopathy).

A homozygous frameshift variant with premature termination, c.6063delC, p.D2021EfsX3, was found in one patient who also harbors p.T1194M and p.T1196I in cis (11-II-1). There have been three *RP1L1* variants in two previous studies found in patients with typical retinitis pigmentosa (RP) caused by homozygous *RP1L1* mutations, namely, c.601delG, p.K203RfsX28; c.1637G>C, p.S546T; and c.1972C>T, p.R658X.^{7,21} In addition, a patient with a cone dystrophy phenotype caused by a homozygous missense mutation, c.3628T>C, p.S1210P, has also been reported.²⁰ Nonsense-mediated decay (NMD) was proposed to explain the fact that mutations in *RP1L1* may cause late-onset autosomal recessive RP.^{7,13} However, the homozygous frameshift variant p.D2021EfsX3 found in our study lies in the nonconserved terminal region. This allele is unlikely to undergo NMD and is distinct from the alleles described in cases with RP. It is difficult to evaluate the clinical impact of the homozygous frameshift variant in our study since multiple variants were found in one patient, although loss of the nonconserved C-terminal region may have little pathogenic impact evident from the prevalence of similar truncating variants in the ExAC dataset. Although genetic and clinical analyses of family members could not be obtained in the present study, further analysis in the future may uncover the clinical impact of the variant.⁷

There were nine patients without pathogenic *RP1L1* variants in this cohort of OMD patients. Eight of these patients lacked at least one of the classical SD-OCT findings, that is, EZ blurring and IZ absence. This indicates that the classical SD-OCT findings can be used to predict whether an OMD patient is carrying a pathogenic *RP1L1* mutation.

Interestingly, p.R1933X of the *RP1* gene and p.Y341X of the *RP2* gene have been identified in patients without pathogenic *RP1L1* variants. There have been two reports describing the p.R1933X variant of the *RP1* gene, where its pathogenicity was interpreted as negative due to nonsegregation with disease and high prevalence in the control group.^{33,34} The other variant, p.Y341X, of the *RP2* gene has never been reported, and its pathogenicity remains uncertain. Further genetic analyses should be designed to investigate the *RP1L1*-negative patients with the occult macular dysfunction syndrome.

Other hereditary disorders should be considered for some of the *RP1L1*-negative patients with occult macular dysfunction syndrome. In 1996, Miyake et al.² first described six sporadic cases that had bilateral central cone dysfunction

resembling familial OMD. Our results support the presence of patients having bilateral progressive maculopathy without family histories or confirmed genetic aberrations.

Overall, our findings suggest two types of pathophysiology associated with bilateral progressive central cone dysfunction with normal fundus (occult macular dysfunction syndrome, Fig. 3). One is a Mendelian hereditary OMD caused by genetic abnormalities such as *RP1L1* mutations (Miyake's disease) and possibly other unknown gene mutations (other OMD). The other type is a retinopathy with clinical signs of occult macular dysfunction syndrome, that is, clinical and ERG findings similar to hereditary OMD but not related to the Mendelian genetic abnormality. We refer to the non-Mendelian form as OMD-like syndrome (progressive occult maculopathy). Our results suggest that the classical SD-OCT findings and autosomal dominant family history, as well as the presence of known *RP1L1* mutations, can help differentiate the two types.

There are limitations in our study. The applied sequencing method, the targeted genes for analysis, and the protocol for pathogenicity prediction may not be completely accurate. Large deletions in the targeted region could have been missed; proper analysis for the repetitive region (presumably around c.3900_4128) was not available with exome sequencing, and genes not listed on RetNet were not analyzed. More comprehensive gene screening including whole-exome analysis for genes with no prior association with inherited retinal disease in those unsolved families, as well as analysis methods such as whole genome sequencing, could help to further determine the genetic aberrations of our cohort—although short-read sequencing technology may still not allow clear delineation of the *RP1L1* repeat region particularly in individuals who may harbor different numbers of repeats on each allele. Although the in silico analysis was useful in predicting the pathogenicity, multilateral approaches including functional analyses should be incorporated in future studies, for example, creating knock-in mice with the identical mutations, protein interaction assays with mutant proteins, and in vitro investigations of induced pluripotent stem cell-derived photoreceptors.

In conclusion, this study investigated the photoreceptor microstructural and molecular genetic characteristics of a Japanese cohort with OMD in a multicenter study. The findings delineated the spectrum of the disorder in both the photoreceptor microstructural phenotype and genotype. The results have highlighted the importance of knowledge of the photoreceptor microstructures for a more accurate diagnosis of the *RP1L1*-associated OMD (Miyake's disease). In addition, the presence of other hereditary disorders, for example, non-*RP1L1* hereditary OMD or non-Mendelian hereditary disorders with mostly nonclassical photoreceptor microstructural findings, an OMD-like syndrome, is implied in the *RP1L1*-negative patients with central cone dysfunction and normal fundus.

Acknowledgments

The authors thank the patients and their families for participation in this study. We thank Duco Hamasaki, PhD, of the Bascom Palmer Eye Institute, University of Miami School of Medicine, Miami, Florida, for discussions and editing of our manuscript.

Supported by research grants from the Japan Agency for Medical Research and Development, the Ministry of Health, Labor and Welfare, and Japan, Grants-in-Aid for Scientific Research, Japan Society for the Promotion of Science. KF is supported by Foundation Fighting Blindness, United States. The authors have no proprietary or commercial interest in any materials discussed in this article.

Disclosure: **K. Fujinami**, None; **S. Kameya**, None; **S. Kikuchi**, None; **S. Ueno**, None; **M. Kondo**, None; **T. Hayashi**, None; **K.**

Shinoda, None; **S. Machida**, None; **K. Kuniyoshi**, None; **Y. Kawamura**, None; **M. Akahori**, None; **K. Yoshitake**, None; **S. Katagiri**, None; **A. Nakanishi**, None; **H. Sakuramoto**, None; **Y. Ozawa**, None; **K. Tsubota**, None; **K. Yamaki**, None; **A. Mizota**, None; **H. Terasaki**, None; **Y. Miyake**, None; **T. Iwata**, None; **K. Tsunoda**, None

References

- Miyake Y, Ichikawa K, Shiose Y, Kawase Y. Hereditary macular dystrophy without visible fundus abnormality. *Am J Ophthalmol*. 1989;108:292-299.
- Miyake Y, Horiguchi M, Tomita N, et al. Occult macular dystrophy. *Am J Ophthalmol*. 1996;122:644-653.
- Miyake Y, Tsunoda K. Occult macular dystrophy. *Jpn J Ophthalmol*. 2015;59:71-80.
- Fujii S, Escano MF, Ishibashi K, Matsuo H, Yamamoto M. Multifocal electroretinography in patients with occult macular dystrophy. *Br J Ophthalmol*. 1999;83:879-880.
- Piao CH, Kondo M, Tanikawa A, Terasaki H, Miyake Y. Multifocal electroretinogram in occult macular dystrophy. *Invest Ophthalmol Vis Sci*. 2000;41:513-517.
- Wildberger H, Niemeyer G, Junghardt A. Multifocal electroretinogram (mfERG) in a family with occult macular dystrophy (OMD). *Klin Monbl Augenbeilkd*. 2003;220:111-115.
- Davidson AE, Sergouniotis PI, Mackay DS, et al. RP1L1 variants are associated with a spectrum of inherited retinal diseases including retinitis pigmentosa and occult macular dystrophy. *Hum Mutat*. 2013;34:506-514.
- Tsunoda K, Usui T, Hatase T, et al. Clinical characteristics of occult macular dystrophy in family with mutation of RP1L1 gene. *Retina*. 2012;32:1135-1147.
- Fujinami K, Tsunoda K, Hanazono G, Shinoda K, Ohde H, Miyake Y. Fundus autofluorescence in autosomal dominant occult macular dystrophy. *Arch Ophthalmol*. 2011;129:597-602.
- Akahori M, Tsunoda K, Miyake Y, et al. Dominant mutations in RP1L1 are responsible for occult macular dystrophy. *Am J Hum Genet*. 2010;87:424-429.
- Conte I, Lestingi M, den Hollander A, et al. Identification and characterisation of the retinitis pigmentosa 1-like1 gene (RP1L1): a novel candidate for retinal degenerations. *Eur J Hum Genet*. 2003;11:155-162.
- Bowne SJ, Daiger SP, Malone KA, et al. Characterization of RP1L1, a highly polymorphic paralog of the retinitis pigmentosa 1 (RP1) gene. *Mol Vis*. 2003;9:129-137.
- Yamashita T, Liu J, Gao J, et al. Essential and synergistic roles of RP1 and RP1L1 in rod photoreceptor axoneme and retinitis pigmentosa. *J Neurosci*. 2009;29:9748-9760.
- Kabuto T, Takahashi H, Goto-Fukuura Y, et al. A new mutation in the RP1L1 gene in a patient with occult macular dystrophy associated with a depolarizing pattern of focal macular electroretinograms. *Mol Vis*. 2012;18:1031-1039.
- Okuno T, Hayashi T, Sugasawa J, et al. Elderly case of pseudo-unilateral occult macular dystrophy with Arg45Trp mutation in RP1L1 gene. *Doc Ophthalmol*. 2013;127:141-146.
- Takahashi H, Hayashi T, Tsuneoka H, et al. Occult macular dystrophy with bilateral chronic subfoveal serous retinal detachment associated with a novel RP1L1 mutation (p.S1199P). *Doc Ophthalmol*. 2014;129:49-56.
- Hayashi T, Gekka T, Kozaki K, et al. Autosomal dominant occult macular dystrophy with an RP1L1 mutation (R45W). *Optom Vis Sci*. 2012;89:684-691.
- Ahn SJ, Cho SI, Ahn J, Park SS, Park KH, Woo SJ. Clinical and genetic characteristics of Korean occult macular dystrophy patients. *Invest Ophthalmol Vis Sci*. 2013;54:4856-4863.
- Ziccardi L, Giannini D, Lombardo G, et al. Multimodal approach to monitoring and investigating cone structure and function in an inherited macular dystrophy. *Am J Ophthalmol*. 2015;160:301-312, e306.
- Kikuchi S, Kameya S, Gocho K, et al. Cone dystrophy in patient with homozygous RP1L1 mutation. *Biomed Res Int*. 2015;2015:545243.
- Oishi M, Oishi A, Gotoh N, et al. Comprehensive molecular diagnosis of a large cohort of Japanese retinitis pigmentosa and Usher syndrome patients by next-generation sequencing. *Invest Ophthalmol Vis Sci*. 2014;55:7369-7375.
- Marmor MF, Fulton AB, Holder GE, et al. ISCEV Standard for full-field clinical electroretinography (2008 update). *Doc Ophthalmol*. 2009;118:69-77.
- McCulloch DL, Marmor MF, Brigell MG, et al. ISCEV Standard for full-field clinical electroretinography (2015 update). *Doc Ophthalmol*. 2015;130:1-12.
- Hood DC, Bach M, Brigell M, et al. ISCEV standard for clinical multifocal electroretinography (mfERG) (2011 edition). *Doc Ophthalmol*. 2012;124:1-13.
- Katagiri S, Yoshitake K, Akahori M, et al. Whole-exome sequencing identifies a novel ALMS1 mutation (p.Q2051X) in two Japanese brothers with Alstrom syndrome. *Mol Vis*. 2013;19:2393-2406.
- Katagiri S, Akahori M, Sergeev Y, et al. Whole exome analysis identifies frequent CNGA1 mutations in Japanese population with autosomal recessive retinitis pigmentosa. *PLoS One*. 2014;9:e108721.
- Li H, Durbin R. Fast and accurate short read alignment with Burrows-Wheeler transform. *Bioinformatics*. 2009;25:1754-1760.
- McKenna A, Hanna M, Banks E, et al. The Genome Analysis Toolkit: a MapReduce framework for analyzing next-generation DNA sequencing data. *Genome Res*. 2010;20:1297-1303.
- Cingolani P, Platts A, Wang le L, et al. A program for annotating and predicting the effects of single nucleotide polymorphisms, SnpEff: SNPs in the genome of *Drosophila melanogaster* strain w1118; iso-2; iso-3. *Fly*. 2012;6:80-92.
- Ng PC, Henikoff S. SIFT: predicting amino acid changes that affect protein function. *Nucleic Acids Res*. 2003;31:3812-3814.
- Adzhubei IA, Schmidt S, Peshkin L, et al. A method and server for predicting damaging missense mutations. *Nat Methods*. 2010;7:248-249.
- Siepel A, Bejerano G, Pedersen JS, et al. Evolutionarily conserved elements in vertebrate, insect, worm, and yeast genomes. *Genome Res*. 2005;15:1034-1050.
- Pollard KS, Hubisz MJ, Rosenbloom KR, Siepel A. Detection of nonneutral substitution rates on mammalian phylogenies. *Genome Res*. 2010;20:110-121.
- Baum L, Chan WM, Yeung KY, Lam DS, Kwok AK, Pang CP. RP1 in Chinese: eight novel variants and evidence that truncation of the extreme C-terminal does not cause retinitis pigmentosa. *Hum Mutat*. 2001;17:436.